Supplementary

Appendix 1

Data details

Table S1 Data for training, validation and testing

Anatomic region	Number of images	Sequence		
Abdomen	96410	Bssfp_2D_Cor	Dgre_Tra	T2_SPAIR_ROKAR Nova
		Bssfp_BH_Cor	DIXON Nova_DYN_W	T2_SPAIR_ROKAR Nova_HR
		Bssfp_Cor	EXCOFEA	T2_TSE_FS_Gated_Tra
		Bssfp2d_2BH	T1_VIGE_Tra	T2_TSE_Gated_Tra
		DANCE	T2_rokar_RT_tra	T2_TSE_SPAIR
		Dgre_2BH	T2_SPAIR	VIGE_BH_Tra
		Dgre_BH_Tra	T2_SPAIR_ROKAR	VIGE_DYN
Joints	15750	PD_TSE_DIXON_Sag	T1_TSE_Sag	T2_TSE_Sag
		PD_VAST_Sag	T1mapping_Sag	T2_TSE_Tra
		Sgre3d_WATEX_Sag	T2_sgre_Sag	T2mapping_Sag
		T1_TSE_Cor		
Head	130280	Brainquant_Tra	T1_SE_Cor	T2_TSE_FLAIR_Tra
		CS_TOF3D	T1_TSE_IR_Tra	T2_TSE_ROKAR Nova_Tra
		MUSIC_Tra	T1_VAST_Sag	T2_TSE_Sag
		SWI_Tra	T2_FLAIR_Tra	T2_TSE_Tra
		T1_IR_TSE_Tra	T2_ROKAR Nova_Tra	T2_VAST_Sag
		T1_MPRAGE_Tra	T2_TSE_Cor	TOF3D
Pelvis	27530	T1_DIXON Nova_DYN_Tra	T1_VIGE_Tra_DYN	T2_TSE_DIXON Nova_Tra
		T1_TSE_Tra	T2_TSE_Cor	T2_TSE_Tra
Spine	14640	Sgre_3D_WATEX_Cor	T2_STIR_Cor	T2_TSE_DIXON Nova
		T1_DIXON_Cor	T2_STIR_Sag	T2_TSE_DIXON Nova_Sag
		T1_TSE_Sag	T2_STRI_Cor	T2_TSE_Sag
		T2_sstse_Cor	T2_STRI_Sag	T2_TSE_STIR_Sag

Data availability statement

The training data used in this study consist of real-world clinical patient images, which are subject to strict institutional policies to protect patient privacy and therefore cannot be publicly shared. However, we recognize the importance of transparency in scientific research and are willing to provide a limited number of de-identified example cases upon reasonable request, subject to institutional approval. This ensures compliance with privacy regulations while facilitating reproducibility of our work.

Model robustness evaluation

Model robustness evaluation on different anatomic regions and imaging sequences

https://dx.doi.org/10.21037/qims-24-1344

We conducted a series of cross-validation experiments to evaluate the robustness of our deep learning model. The model was trained on a small-scale training set comprising magnetic resonance imaging (MRI) images of specific anatomical regions and imaging sequences, with the aim of removing Gibbs artifacts from MRI images of T1 SE Axial, T2 TSE Axial, T2 TSE FLAIR Axial, T2 TSE Sagittal, and T2 TSE Coronal sequences of the head, abdomen, spine, pelvis, and joints. To evaluate the robustness of the proposed model, we trained two models for each anatomical region and imaging sequence, using different training sets. One training set contained images of all regions, while the other contained only images of the region of interest. We tested both models on the same test set and compared their outputs with the original images to verify the robustness and generalization ability of the proposed model.

Table S2 Test experiments for model robustness evaluation on different anatomic regions and imaging sequences

Test experiment	Training set	Test set
Abdomen	Model 1: 200 images each of head, spine, pelvis, and Joints; Model 2: 800 images of abdomen	200 Abdomen images
Head	Model 1: 200 images each of abdomen, spine, pelvis, and Joints; Model 2: 800 images of head	200 Head images
Spine	Model 1: 200 images each of abdomen, head, pelvis, and Joints; Model 2: 800 images of spine	200 Spine images
Pelvis	Model 1: 200 images each of abdomen, head, spine, and Joints; Model 2: 800 images of pelvis	200 Pelvis images
Joints	Model 1: 200 images each of abdomen, head, spine, and pelvis; Model 2: 800 images of Joints	200 Joints images
T1 SE Axial	Model 1: 200 images each of T2 TSE Axial, T2 TSE FLAIR Axial, T2 TSE Sagittal, and T2 TSE Coronal; Model 2: 800 images of T1 SE Axial	200 T1 SE Axial images
T2 TSE Axial	Model 1: 200 images each of T1 SE Axial, T2 TSE FLAIR Axial, T2 TSE Sagittal, and T2 TSE Coronal; Model 2: 800 images of T2 TSE Axial	200 T2 TSE Axial images
T2 TSE FLAIR Axial	Model 1: 200 images each of T1 SE Axial, T2 TSE Axial, T2 TSE Sagittal, and T2 TSE Coronal; Model 2: 800 images of T2 TSE FLAIR Axial	200 T2 TSE FLAIR Axial images
T2 TSE Sagittal	Model 1: 200 images each of T1 SE Axial, T2 TSE Axial, T2 TSE FLAIR Axial, and T2 TSE Coronal; Model 2: 800 images of T2 TSE Sagittal	200 T2 TSE Sagittal images
T2 TSE Coronal	Model 1: 200 images each of T1 SE Axial, T2 TSE Axial, T2 TSE FLAIR Axial, and T2 TSE Sagittal; Model 2: 800 images of T2 TSE Coronal	200 T2 TSE Coronal images

Model robustness evaluation on different severity of Gibbs artifacts

To assess the robustness of the proposed model on different Gibbs artifact severity, we sampled 100 cases from three anatomical regions, namely the head, spine, and abdomen, as the label. Next, the Gibbs artifact generator algorithm was applied to these images at various frequency positions, resulting in five sets of images containing a total of 500 images with different severity of Gibbs artifacts. The intensity of Gibbs artifacts in each image was quantified using both the labeled images and the images containing Gibbs artifacts. A novel index, termed Gibbs Artifact Intensity (GAI, see below), was

https://dx.doi.org/10.21037/qims-24-1344

developed to provide a quantitative evaluation of the severity of Gibbs artifacts in the images. Subsequently, GibbsCut was employed to remove the Gibbs artifacts in the 500 images, resulting in 500 output images. The differences between the label images and the output images were quantified by calculating the mean squared error (MSE) for each image. Finally, we used Pearson correlation analysis to evaluate the correlations between GAI and MSE for different anatomical regions.

Quantification of Gibbs artifact intensity

To conduct an objective analysis of the impact of Gibbs artifact intensity on algorithm performance, we first established a definition of Gibbs artifact intensity and develop a methodology to measure it. To quantitatively assess the severity of Gibbs artifacts in an image, it is necessary to identify which signals in the image correspond to Gibbs artifact signals. Therefore, as depicted in *Figure S1*, a labeled image without Gibbs artifacts and a corresponding image containing Gibbs artifacts (i.e., original image) are required. The labeled image was then subtracted from the original image to produce a residual image, which primarily consisted of Gibbs artifact signals.

We constructed an index, namely GAI, for quantitative measurements of the severity of the Gibbs artifacts present in each image. Firstly, we subtracted the original image with Gibbs artifact from the label image without Gibbs artifact to obtain the residual image. The residual image represented the Gibbs artifact signal. The energy of the Gibbs artifact signal between the original image X and the label image Y (the energy of the difference between the two images) is calculated using the following formula:

$$E = \sum_{i=1}^{H} \sum_{j=1}^{W} \left(X(i,j) - Y(i,j) \right)^2 \quad [1]$$

Where E represents the energy of the Gibbs artifact signal, $X(i,j)$ And $Y(i,j)$ Represent the pixel values at the corresponding coordinates on the image, and H and W are the height and width of the image, respectively. The GAI formula is defined as follows:

$$\mathrm{GAI} = \frac{E}{\sum_{i=1}^{H} \sum_{j=1}^{W} \left(Y(i,j) \right)^2} \quad [2]$$

The GAI represents the relative ratio of the Gibbs artifact signal energy and the image signal energy. A smaller value of GAI indicates a lower Gibbs artifact severity in the image, making it a useful metric for quantitatively evaluating the intensity of Gibbs artifacts in an image.

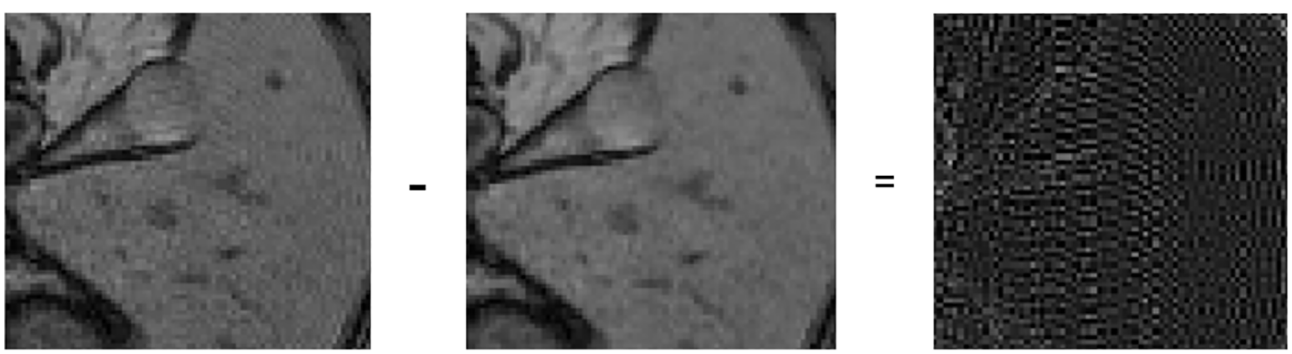

Figure S1 The residual image used to quantify the severity of Gibbs artifacts is obtained by subtracting the label image from the original image.

https://dx.doi.org/10.21037/qims-24-1344

Image quality and model robustness assessment

Table S3 Analysis of variance of image quality score of MRI images processed by different artifact removal methods

Dataset	Anatomic region	Image group				P value
		Original	Tukey	GEA	GibbsCut	
Internal testing set	Head	2.86±0.43	3.56±0.74	3.52±0.55	4.12±0.42	<0.001
	Spine	2.64±0.54	3.14±0.52	3.27±0.60	3.91±0.50	<0.001
	Abdomen	2.45±0.58	3.22±0.71	3.16±0.65	3.87±0.72	<0.001
External testing set	Head	2.63±0.59	3.39±0.43	3.26±0.52	3.96±0.45	<0.001
	Spine	2.61±0.52	3.50±0.48	3.19±0.46	4.10±0.45	<0.001
	Abdomen	2.88±0.53	3.19±0.57	3.30±0.54	3.62±0.49	<0.001

The value is presented as means ± SD. GEA, Gibbs elimination algorithm.

Table S4 Analysis of variance of image quality score in cross validation for MRI sequences

Sequence	Image group			P value
	Original	Model 1	Model 2	
T1 SE Axial	3.10±0.50	4.39±0.51	4.39±0.64	0.002
T2 TSE Axial	2.83±0.29	4.29±0.51	4.19±0.50	<0.001
T2 TSE FLAIR Axial	2.63±0.56	4.33±0.71	4.30±0.30	<0.001
T2 TSE Sagittal	2.72±0.70	4.34±0.46	4.29±0.53	<0.001
T2 TSE Coronal	2.97±0.62	4.27±0.42	4.28±0.55	<0.001

The value is presented as means ± SD.

Table S5 Analysis of variance of image quality score in cross validation for anatomic regions

Anatomic region	Image group			P value
	Original	Model 1	Model 2	
Head	2.81±0.72	4.29±0.71	4.32±0.74	<0.001
Spine	2.80±0.34	4.33±0.46	4.46±0.51	<0.001
Abdomen	2.57±0.54	4.45±0.38	4.47±0.35	<0.001
Pelvis	2.92±0.61	4.30±0.56	4.28±0.73	<0.001
Joints	2.80±0.59	4.27±0.39	4.27±0.68	0.001

The value is presented as means ± SD.

https://dx.doi.org/10.21037/qims-24-1344